Geotechnical Aspects of Underground Construction in Soft Ground – Viggiani (ed)
© 2012 Taylor & Francis Group, London, ISBN 978-0-415-68367-8

Spatial effects on excavations in deep soft lacustrine clay

P. Becker
University of Strathclyde, Glasgow, Scotland

G. Berhane
Ed. Zueblin AG, Stuttgart, Germany

H.-G. Kempfert
University of Kassel, Germany

ABSTRACT: A case history of a deep excavation in Constance near the lake Constance north of the German Alps is presented in this paper. The excavation was 90 m long, 17.5 to 22.5 m wide and 6 m deep. The underground condition in Constance and the surroundings is known of a deep and soft deposit of lacustrine clay. The spatial effects on the excavation, specially the effects of the construction steps on the deformation behaviour as well as the mobilization of each support element, has been studied by means of back analyses using the Finite Element Method (FEM) with 2D-models. The computed results are compared with the measured data from the project with respect to the time dependency of the soil-structure-interaction and deformation behaviour. For this purpose, additional pore pressure sensors were installed to record the development of excess pore pressure corresponding to different construction stages. Finally, recommendations on numerical modelling of excavations in soft soils are presented, and mobilization factors for support elements and the stress path dependant stiffness of soft soils are described.

1 INTRODUCTION

Prediction of deformations resulted from excavations in soft soils is generally performed using the Finite Element Method (FEM) and with the application of advanced constitutive soil models. A reliable estimation of deformations in advance of the project is generally not possible due to the variety of factors on soil-structure-interaction (see Becker 2009). Rather the FEM is applied at excavations in soft soils for more than three decades in conjunction with the observation method. The numerical calculation leads with variations of the material parameters to both alarm and limit values of deformations and forces, taking into account a realistic modelling of the boundary value problem.

The time-dependent material behaviour and the characteristic stress paths in excavations, which differ from those of standard laboratory tests, require a high degree of experience of the geotechnical engineer for estimating the material parameters. If there are no appropriate laboratory test results and calibration of measuring results in the planning phase is not yet possible, uncertainties regarding the numerical deformation prediction increase significantly and hamper as well the design of structures and the optimization of the construction process. In the following numerical analysis of a case study, the stress-strain behaviour of soft soils depending on stress-paths due to the excavation process is considered using a commercially available FE-Program and advanced constitutive soil models.

2 GENERAL DESCRIPTION OF THE EXCAVATION SITE

2.1 *Support system and construction stages*

The case history is located in southern Germany at Lake Constance. The construction work for the 5-storey building with a length of 87.5 m and a width between 17.5 and 22.5 m began in the summer of 2007. A site plan of the excavation is shown in Figure 1.

The excavation is 5.90 m deep and it is supported by a secant bored pile wall. The piles have a diameter $D = 1.07$ m and a pile length $l = 10.5$ m. The bored pile wall was reinforced by a concrete beam wale at the top all around, which gives the wall additional strength in the longitudinal direction of the excavation pit previous to the installation of the struts.

The construction sequence is shown in Figure 2. The excavation was conducted in slices from a preliminary excavation level at depth of −1.50 m

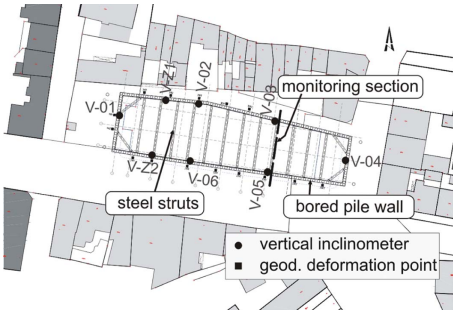

Figure 1. Site plan with monitoring section.

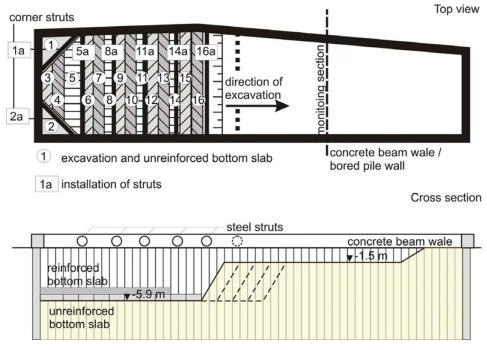

Figure 2. Top view and cross section of the excavation site with idealized construction stages.

below the surface. The excavation was started at the two Western corners making use of the spatial support of bored pile wall and upper concrete beam wale. Immediately after the excavation a triangular-shaped unreinforced bottom slab (d = 50 cm) was placed. Diagonal steel tube struts with a diameter D = 80 cm were installed afterwards at the corners. Thereafter, the excavation proceeded with a sloped trench of 2 m width and immediate placement of unreinforced bottom slabs in daily time basis. With the progress of the excavation and reaching the entire excavation width, the first steel tube strut with a diameter D = 76 cm was installed (step 5a in Fig. 2).

After each further excavation in slices over the entire width of the excavation, unreinforced bottom slabs were placed and the struts installed at a centre to centre distance of 6.9 m. Finally, a reinforced bottom slab was casted on the top of the unreinforced bottom slab (Fig. 2).

2.2 *Underground condition*

The soil investigation was conducted using bore holes and cone penetration tests. Additional information on the underground was also available from previous excavation sites in direct surrounding, see for e.g. Becker et al. (2008) and Kempfert & Gebreselassie (2006).

The ground consists of 5 layers (Fig. 3). The upper most layer is 2.0 m thick fill material. Beneath the fill is a 10.0 to 26.0 m thick soft lacustrine clay deposit which is divided into 2 layers. The upper lacustrine clay has predominantly soft consistency whereas the lower lacustrine clay has a soft to stiff consistency due its sand and gravel contents. Beneath the lacustrine clay layers is a 7.0 to 10.0 m thick transient layer with predominantly sand and silt content and a variable content of gravel particles. From a depth of –19 m in the west and –37 m in the east downwards, the underground is dominated by a ground moraine.

2.3 *Monitoring*

The excavation was accompanied by the observation method. In particular seven vertical inclinometers and twenty geodetic deformation points were installed (Fig. 1). Moreover, pore pressure transducers were installed into at a specified monitoring section (Fig. 1). In Figure 4 is the layout of the pore pressure transducers in the monitoring section shown. For more details about the instrumentation refer to Becker (2009).

2.4 *Measurement results*

The measurement results are discussed for the monitoring section defined in Figure 1. Due to the limitation of the length of this paper, the measurements results are shown in section 4 of this paper in connection with numerical analysis results. For more information refer to Becker (2009).

The time dependant and spatial influence of slice wise excavation on the horizontal wall displacements at the upper concrete beam wale is identified by the evaluation of the geodetic deformation measurements (Fig. 11). At measuring point 3301 the first deformations were recorded 20 days prior to the execution of the corresponding excavation slice on 02.11.2007.

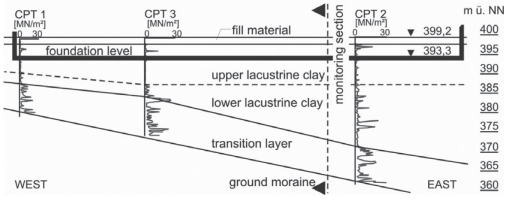

Figure 3. Underground condition in West–East cross section.

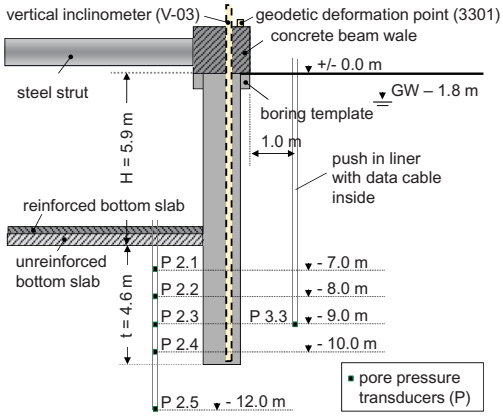

Figure 4. Monitoring section through bored pile wall showing pore pressure transducers, vertical inclinometer and geodetic deformation point.

The vertical inclinometer measurements at the monitoring section are shown in Figure 10. In the left chart are the measurements from the southern bored pile wall (V-06 and V-05) and in the right chart are from the northern side (V-02 and V-03). The horizontal displacements on the southern side (V-06 and V-05) show a uniform distribution with maximum values of 9 mm at the wall head and 12.5 mm to 14 mm at the wall toe. The deformation of the opposite northern side (V-02 and V-03), however, vary between 5 mm and 11 mm at the wall head and between 7.5 and 17 mm at the wall toe. The maximum displacement ratio $u_h/H = 0.25\%$ is very moderate and it is support system dependant. For further deformation measurements, see Becker (2009).

The time-dependent development of excess pore pressure is shown in Figure 12. The excavation of the slice at the location of the monitoring section was done on 02.11.2007. As a result of the stress relief due to the excavation, an excess pore pressure change of 48 kN/m² occurred at all measuring points in front of the wall toe. Influence of wall deformation on excess pore pressure was not observed. Afterwards, a slight increase of excess pore pressure was observed due to the consolidation process. The installation of the reinforced bottom slab resulted in a sudden increase of the excess pore pressure by an amount of 10 kN/m².

3 SPATIAL EFFECTS ON STIFFNESS OF SOFT SOILS

3.1 *Stress path dependant stiffness*

It is well known that the stiffness of soils is dependent on the applied stress path, e.g. primary loading and un-/reloading, see also Parry (1995), Gebreselassie (2003) and Powrie et al. (1998). Furthermore, the dependency of the stiffness of soft soils on stress paths due to excavation is investigated by Becker (2009). The stiffness of the soil from stress path tests differs significantly from standard laboratory tests. Figure 5 shows idealized stress paths in excavations, which were analysed for soft soils. The stress path D (TSP-D) is typical for stress condition in the centre direct below the excavation bottom. The influence of horizontal stresses due to wall deformations increases with approaching the retaining structure and the stress path turns anticlockwise and corresponds to the stress path TSP-F.

A summary of the stiffness ratios of the secant modulus E_{50} for soft lacustrine clays are shown in Table 1.

3.2 *Numerical modelling of stress-strain behaviour of soft soils*

Characteristic stress path zones (SPZ) in excavations in soft soils for different construction phases

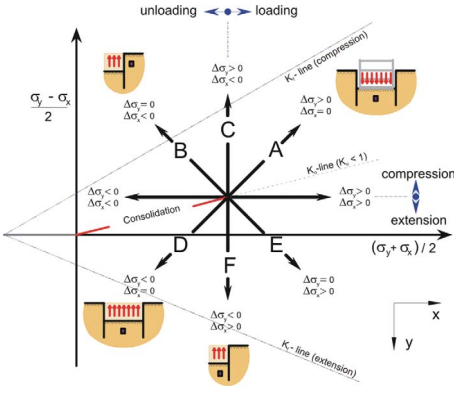

Figure 5. Idealized stress paths for triaxial tests.

Table 1. Influence of stress paths on stiffness of soft lacustrine clays, after Becker (2009).

	$f_{TSP} = E_{50,TSP-I}/E_{50,TSP-A}$			
Stress path	Lacustrine clay[1]	Lacustrine clay[2]	Kaolin	Average
TSP-A	1.0	1.0	1.0	1.0
TSP-B	9.0	5.1	1.2	5.1
TSP-D	7.8	1.3	3.4	4.2
TSP-E	5.3	2.9	3.2	3.8
TSP-F	8.7	4.2	–	6.5

[1]from this case history; [2]from a different case history (to be published soon).

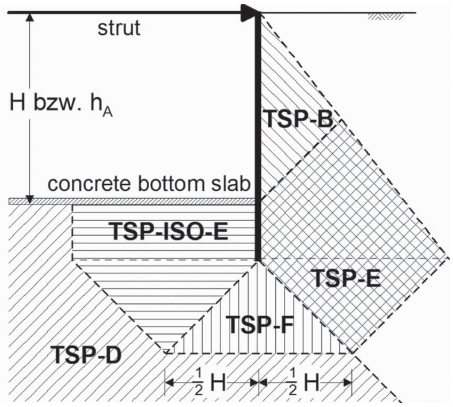

Figure 6. Characteristic stress path zones (SPZ).

have been identified as a result of a numerical parameter study by Becker (2009). In Figure 6 is the SPZ together with the corresponding total stress paths depending on the construction stage and the resulting soil structure interaction shown for a retaining wall with support at the top with strut and at the bottom with concrete bottom slab. For additional SPZ's at different construction phases see Becker (2009).

4 NUMERICAL BACK ANALYSIS

4.1 *General*

The 2D numerical analysis was performed for the monitoring section indicated in Figure 1. The spatial influences of soil structure interaction on the deformation behaviour, e.g. slice wise excavation, installation of supporting bottom slab and steel struts, are considered in the analysis using an idealized modelling of the construction progress. The time-dependent behaviour was considered with the help of an undrained analysis using a coupled consolidation analysis which take into account the actual construction periods.

The numerical calculation was made using the FEM program PLAXIS v9. The elasto plastic Hardening Soil model (HS) and also the Hardening Soil Small model (HSS) were applied as constitutive soil models. For detailed information's about the soil models see Schanz (1998), Brinkgreve et al. (2004, 2008) and Benz (2007).

4.2 *FE model geometry and idealisation of spatial effects*

At the monitoring section is the excavation width B = 21.4 m and the excavation depth H = 5.9 m. The FE model has a width of 2.5.B = 54.5 m on both sides of the excavation and has a height of 50 m (Fig. 7).

The constructive elements were modelled with both continuum and structural elements. The bored pile wall was idealized as linear elastic continuum elements. Additionally a linear elastic beam is arranged at the axis of the bored pile wall, which was used for estimating the section forces. The bending stiffness of the beam element did not affect the bored pile wall stiffness, because of $EI_{Beam} \approx 0$. The section forces of the beam element are then be multiplied with an adjustment factor f depending on the stiffness ratio according to Equation 1.

The unreinforced and the reinforced bottom slabs with thickness d = 0.75 m and d = 0.80 m respectively are discretised using continuum elements. The upper concrete beam wale was idealised with an additional load which is equal to its weight. The supporting effect of the concrete beam wale was idealised using different activation stages of the upper steel struts (see also section 4.3).

$$f = \frac{EI_{continuum} + EI_{Beam}}{EI_{Beam}} \tag{1}$$

4.3 *Calculation phases*

The real construction process of the excavation at the monitoring section has been distributed to a longer period to take account of temporal effects on the stress deformation behaviour and was related to excess pore pressure measurements.

The main difficulty in a 2D analysis is to model the spatial effects of the supporting structures. For this case study, this is the slice wise construction of the bottom slab and the installation of the steel struts. These effects were examined separately in a numerical analysis. Figure 8 shows the idealized

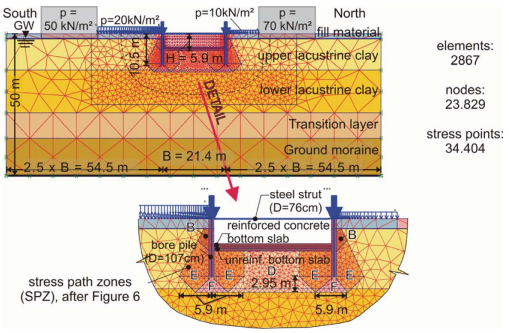

Figure 7. FE geometry model with characteristic Stress Path Zones (SPZ) in detail.

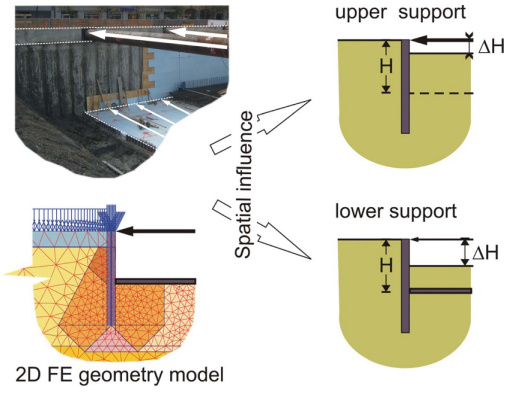

Figure 8. Idealization of spatial effects considering upper and lower support of the retaining wall.

model which take into account the upper and lower supporting structures.

The spatial effect of the steel struts in conjunction with the bending stiffness of the upper concrete beam wale was analysed using a mobilisation factor f_{mob} according to Equation 2 and Figure 8. Here, ΔH is the excavation depth before the installation of the support element and H is the full excavation depth.

The spatial effect of the bottom slab in conjunction with the slice wise excavation and the remaining support from the soil, which is still to be excavated, was also analysed using the mobilisation factor f_{mob}.

$$f_{mob} = \frac{\Delta H}{H} \tag{2}$$

The calculation phases are summarized in Table 2. For all calculation steps a groundwater flow calculation was carried out with a water table at a depth of −1.8 m behind the wall and at the bottom of excavation within the excavation. The above mentioned spatial effects were considered at the calculation phases 04 and 07. This changed the calculation phase in a purely plastic calculation and soil excavation was controlled by the program's internal factor m_{stage}, which reduces the stiffness of the excavation area, see also Schikora & Fink (1982) and Lackner (2008). The partial excavation depth H_i can be approximately determined using Equation 3. The subsequent calculation step was performed using a coupled consolidation analysis taking into account the conceptual construction period of the previous step, where the partial calculation step ($m_{stage} < 1.0$) has been completed.

$$H_i = m_{stage} \cdot \Delta H \tag{3}$$

Table 2. Calculation phases.

Phase	Type	Description	Time [d]
00	P	Initial stress (K_0-procedure)	
01	P	Activation of surcharge load	
02	C	Installation of bored pile wall (whished-in-place)	10
03	C	Activation of upper concrete beam (additional load)	5
04	C[1]	1st excavation step –1.0 m	5
05	P	Installation of upper struts	
06	C	2nd excavation step –2.0 m	4
07	C[1]	3rd excavation step –5.9 m	11
08	P	Installation of lower concrete slap	
09	C	Consolidation	9
10	P	Construction of reinforced concrete slap	10
11	C	Consolidation (min pore pressure)	

N.B.: P—plastic calculation; C—plastic consolidation with coupled consolidation analysis; [1]Calculation with m_{stage} 1.0 plastic (P) and following phase was plastic consolidation (C).

4.4 *Material parameters*

The material parameters for the relevant upper lacustrine clay layer were determined from laboratory tests (Becker 2009). The parameters of the remaining soil layers were adopted from geotechnical reports and verified by parameters from adjacent projects. The additional Hardening Soil Small (HSS) model parameters were estimated based on Benz's (2007) empirical correlations. In Table 3 are the material parameters for the HS model and in Table 4 for HSS model.

The material parameters of the structural elements are indicated in Table 5 and of the continuum elements in Table 6.

Taking into account the stress path dependent stiffness in the characteristic stress path zones (SPZ) according to Table 1 the modified stiffness are summarized in Table 7. Here, the stiffness was increased with the stiffness ratios f_{TSP} from the average values for each stress path zone respectively.

4.5 *Comparison with measurement results*

Before the comparison of the numerical calculations with the measurement results the spatial influence of the supporting elements and the stress path dependant stiffness is discussed. The results of variation of the mobilisation factor $f_{mob,F}$ which represents the idealisation of the supporting bottom slab are presented exemplary. The mobilisation factor for the upper steel strut is kept constant with $f_{mob,K} = 0.017$ throughout this analysis.

Table 3. Soil parameters for the HS-model.

Soil layer	γ_{sat} [kN/m³]		γ_{unsat} [kN/m³]		$k_x = k_y$ [m/d]	
a) Unit weight and permeability						
Fill material	20.0		20.0		8.64E-2	
Upper lacustrine clay	19.0		19.0		8.64E-4	
Lower lacustrine clay	19.0		19.0		8.64E-4	
Transition layer	20.0		20.0		8.60E-4	
Ground moraine	22.0		22.0		8.60E-4	
	E_{50}^{ref} [MN/m²]	G_0^{ref} do.	E_{ur}^{ref} do.	p^{ref} do.	ν_{ur} [–]	m [–]
b) Stiffness parameters						
Fill material	3.0	3.0	12.0	0.1	0.2	0.60
Upper lacustrine clay	5.9	4.5	19.0	0.1	0.2	0.90
Lower lacustrine clay	6.0	5.5	24.0	0.1	0.2	0.90
Transition layer	8.0	8.0	32.0	0.1	0.2	0.80
Ground moraine	30.0	30.0	120.0	0.1	0.2	0.75
	c′ [kN/m²]	φ′ [°]		ψ′ [°]		Rf [–]
c) Shear strength parameters						
Fill material	0.01	27.5		0.0	0.90	
Upper lacustrine clay	0.01	27.5		0.0	0.90	
Lower lacustrine clay	0.01	25.0		0.0	0.90	
Transition layer	0.01	27.5		0.0	0.90	
Ground moraine	10.00	27.5		0.0	0.90	

Table 4. Additional soil parameters for the HSS-model.

Soil layer	G_0^{ref} [MN/m²]	$\gamma_{0.7}$ [–]
Fill material	35.0	4.2E-04
Upper lacustrine clay	33.0	3.0E-04
Lower lacustrine clay	55.0	2.0E-04
Transition layer	60.0	2.4E-04
Ground moraine	140.0	1.0E-04

Table 5. Material properties of the structural elements.

Structural element	EA [kN/m]	EI [kNm²/m]	w [kN/m/m]	ν [–]
Steel strut (D = 76.2 cm)	7.088E05	5.011E04	0.27	0.3
Bored pile	0.01	0.01	0	0

Table 6. Material properties of the continuum elements.

Continuum element (non-porous)	γ kN/m³	$k_x = k_y$ m/d	ν	E_{ref} MN/m²
Unreinforced bottom slab (d = 0,50 m)	23.0	0	0.20	2.5E04
Reinforced bottom slab (d = 0,80 m)	25.0	0	0.20	3.2E04
Bored piles (D = 1,50 m)	25.0	0	0.20	2.5E04

Table 7. Modified stress path dependant stiffness.

SPZ	f_{TSP}	E_{50}^{ref} [MN/m²]	E_{ur}^{ref} [MN/m²]	G_0^{ref} [MN/m²]	$\gamma_{0,7}$ [–]
B	5.1	16.23	48.80	48.80	3.0E-04
D	4.2	13.40	40.20	40.20	3.6E-04
E	3.8	12.12	36.36	36.36	4.0E-04
F	6.5	20.74	62.21	62.21	2.4E-04

The spatial effects of installing the bottom slab at different mobilisation factors on the wall deformation are shown in Figure 9. The computation results using the HS-model (standard) confirm the difficulties of prediction of the deformations in excavation in soft soils. Here, the material parameters are taken from standard triaxial tests and the excavation depths are modelled with realistic assumptions. Similar results had been achieved for the HSS model. In this case, the calculated deformations can only

approach the measurement results if one assumes an excavation level at –2.25 m, i.e. $f_{mob,F} = 0.38$. This excavation depth seems to be rather unrealistic in view of the construction process. In addition, a very high sensitivity to the displacements at the wall toe was observed for both soil models due to the low stiffness in the area of the wall toe.

By taking into account the modified stiffness in characteristic Stress Path Zones (SPZ) the above mentioned sensitivity disappeared. The calculated deformation with the HS-model could approach the measurement results only at a very low mobilisation factor with $f_{mob,F} = 0.38$, which results in an overestimation of the displacements at the head of the wall by 33%. For the HSS-model the best match was found with a mobilisation of the bottom slab from an excavation depth –3.95 m to –4.45 m ($f_{mob,F} = 0.67$ to 0.75). In another comparative calculation, which is not shown here, and that enabled the head reinforcement after an excavation of –0.50 m ($f_{mob,K} = 0{,}085$), no effect on the displacements was found at the toe of the wall, but a corresponding reduction in wall displacements at the head of the wall was observed.

In the following the numerical results using the HSS-model with stress path dependant stiffness in characteristic stress path zones and using the optimized mobilization factors of $f_{mob,K} = 1/6$ and $f_{mob,F} = 2 / 3$ are presented. The mobilisation factors correspond to an excavation depth at - 1.0 m for activating the steel strut and an excavation depth at - 3.95 m for activating the bottom slab.

In Figure 11 the measured wall deformations are compared to the numerical results. With the identified mobilization factors and the modified stress path dependant stiffness, the deformation behaviour can be described very well as expected. In particular a good match between measured and computed toe and head displacements was achieved. The comparison of the numerical results with the results of the vertical inclinometer V-03 on the northern side of the monitoring section can be neglected, because there was some problems in the orientation of this inclinometer. On the other hand, there is a good agreement with the nearby inclinometer V-02.

The spatial effects on the deformation behaviour of excavations in soft soils could be identified for the conducted optimized calculation with modified stress path dependant stiffness and an optimised and realistic idealisation of the excavation steps. Furthermore, the time dependant effects had been analysed as shown in the following figures. The displacements at the head of the wall depending on the construction progress are shown in Figure 11. The numerical results confirm the time dependant increase of the wall head deformations at the measuring point 3301 due to the application of coupled consolidation analysis. In particular the time dependant increase of horizontal displacements after the excavation the slice (02.11.2007) along the monitoring section could be captured after some selected idealisations had been made. In addition, computation results using the HS-model are shown in Figure 11, which takes into account the modified stiffness. After the installation of the steel strut support the results were overrated with the HS-model and could not be approximated afterwards.

The measured time-dependent excess pore pressure development shown in Figure 12 can be described well by the numerical analysis. The calculated excess pore pressure varies depending on the position (Fig. 4), whereas the measurement results describe a uniform pore water pressure $\Delta u \approx -48$ kN/m^2. The measured pore water pressure matches the corresponding effective stress due to the vertical stress relief.

The subsequent consolidation is accelerated considerably by reloading the underground due to the unreinforced bottom slab and in particular the reinforced bottom slab.

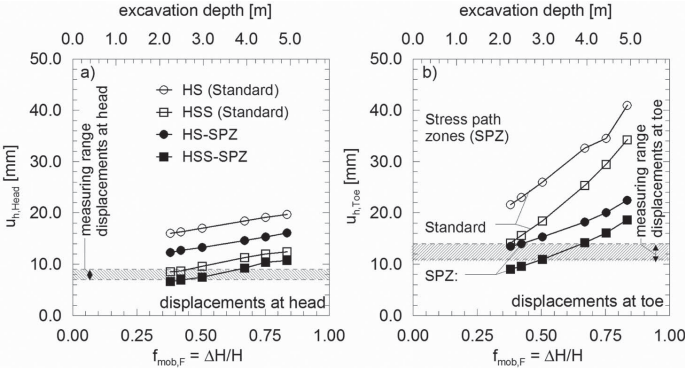

Figure 9. Influence of the mobilisation factor $f_{mob,F}$ on horizontal displacements at the top (a) and the bottom (b) of the bored pile wall.

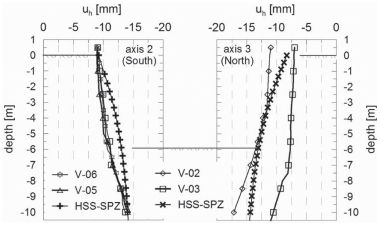

Figure 10. Comparison of calculated horizontal wall displacements with measurement results.

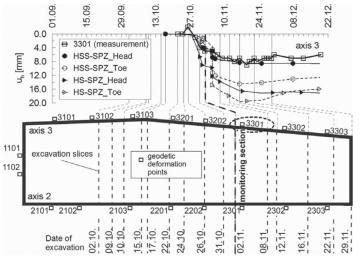

Figure 11. Comparison of calculated horizontal displacements at upper concrete beam wale with measurement results.

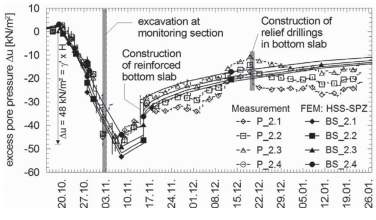

Figure 12. Comparison of calculated excess pore pressures with measurement results.

5 CONCLUSION

The described case study shows very clearly the benefits of a stiff retaining wall in combination with an upper concrete beam wale that can be placed in advance of the excavation. The measurement results inside and outside the excavation area are well below commonly expected values in excavation in soft soils. Although the relevant upper lacustrine clay layer stiffness for this project are slightly higher than in the neighbouring case studies, the selected excavation procedure has prove to be a very good solution for the succesfully completion of excavations in soft soils.

The numerical analysis of the case study confirms the need to take into account the stress path dependent material parameters in the calculation of excavations in soft soils. It was shown that without such optimization technique a successful deformation prediction taking into account a realistic construction process is not possible, neither with Hardening Soil model nor with the Hardening Soil Small model is possible. Taking into account the stress path dependent stiffness in characteristic stress path zones (Becker 2009) resulted in a significant improvement of the numerical prediction of deformations.

The spatial influence of soil-structure interaction designated for this project is considered successfully by idealisation of the upper steel struts and the slice wise excavation and placement of the lower bottom slab with mobilization factors in a two-dimensional numerical analysis. An optimized deformation prediction can be achieved with this method which takes into account the stress path dependent stiffness behaviour when using soil models with isotropic material properties. Application of the Hardening Soil Small model led to a good match with the measurement results.

REFERENCES

Becker, P. 2009. Zeit- und spannungspfadabhängiges Verformungsverhalten bei Baugruben in weichen Böden. Schriftenreihe Geotechnik, Heft 22, Universität Kassel.

Becker, P.; Gebreselassie, B. & Kempfert, H.-G. 2008. Back analysis of a deep excavation in soft lacustrine clays. *6th International Conference on Case Histories in Geotechnical Engineering*. Arlington, Virginia, USA 2008 (Paper 5.17; CD-ROM).

Benz, T. 2007. *Small strain stiffness of soils and its numerical consequences.* Universität Stuttgart. Mitteilung des Institutes für Geotechnik, Heft 55.

Brinkgreve, R.B.J.; Broere, W. & Waterman, D. 2004: *Plaxis—Finite Element Code for Soil and Rock Analyses*. Rotterdam.

Brinkgreve, R.B.J.; Broere, W. & Waterman, D. 2004. *Plaxis—Manual*.

Gebreselassie, B. 2003. Experimental, Analytical and Numerical Investigations of Excavations in Normally Consolidated Soft Soils. Schriftenreihe Geotechnik, Universität Kassel, Heft 14.

Kempfert, H.-G. & Gebreselassie, B. 2006. *Excavations and Foundations in Soft Soils*. Springer Verlag, Berlin.

Lackner, C. 2008. Numerical Simulation of Geosynthetic Reinforced Embankments. *Proc. of the 19th European Young Geotechnical Engineers Conference,* Györ, Hungary, pp. 207–215.

Parry, R.H.G. 1995. *Mohr Circles, Stress Paths and Geotechnics*. E & FN Spon, London.

Powrie, W.; Pantelidou, H. & Stallebrass, S.E. 1998. Soil stiffness in stress paths relevant to diaphragm walls in clay. *Géotechnique 48*, No. 4, pp. 483–494.

Schanz, T. 1998. *Zur Modellierung des mechanischen Verhaltens von Reibungsmaterialien.* Universität Stuttgart, Mitteilung des Inst. f. Geotechnik, Heft 45.

Schikora, K. & Fink, T. 1982. Berechnungsmethoden moderner bergmännischer Bauweisen beim U-Bahn-Bau. *Bauingenieur 57*, S. 193–198.